Available online at www.sciencedirect.com
SCIENCE DIRECT®
Journal of Photochemistry and Photobiology A: Chemistry 166 (2004) 57–62
Journal of Photochemistry and Photobiology A:Chemistry
www.elsevier.com/locate/jphotochem

Porphyrin and fullerene-based photovoltaic devices

Hiroshi Imahori [a,b,*], Makoto Kimura [c], Kohei Hosomizu [a], Shunichi Fukuzumi [c,1]

[a] *Department of Molecular Engineering, Graduate School of Engineering, Kyoto University, PRESTO, Japan Science and Technology Agency (JST), Katsura, Nishikyo-ku, Kyoto 615-8510, Japan*
[b] *Fukui Institute for Fundamental Chemistry, Kyoto University, 34-4, Takano-Nishihiraki-cho, Sakyo-ku, Kyoto 606-8103, Japan*
[c] *Department of Material and Life Science, Graduate School of Engineering, Osaka University, CREST, Japan Science and Technology Agency (JST), Suita, Osaka 565-0871, Japan*

Received 22 October 2003; received in revised form 2 December 2003; accepted 5 April 2004

Abstract

We have developed molecular photovoltaic devices where fullerenes and porphyrins as building blocks are self-assembled onto an ITO electrode. Anodic photocurrent generation was observed when the ITO electrode modified with porphyrin–fullerene dyads was illuminated in the presence of ascorbic acid (AsA) as an electron sacrificer. Photoinduced multistep electron transfer mechanism at the ITO surface is proposed for the photocurrent generation. These results provide basic information for the development of nanostructured molecular photovoltaic devices.

Keywords: Porphyrin; Fullerene; Electron transfer; Self-assembled monolayers; Photovoltaic devices

1. Introduction

Significant efforts have been made in recent years to explore the photoelectrochemical and photovoltaic properties of donor–acceptor systems [1–12]. Since covalently linked donor–acceptor arrays can produce a long-lived, charge-separated state with a high quantum yield, they have been frequently employed in organized systems [1–12]. However, an efficient conversion of light to electrical or chemical energies via the charge-separated state has often been hampered by the poor vectorial electron flow in the covalently linked molecules incorporated into lipid bilayers and Langmuir–Blodgett membranes or organized at electrodes [1–16].

Self-assembled monolayers (SAMs) [17] of donor–acceptor-linked systems are highly promising methodology for the construction of molecular photovoltaic devices, because donor–acceptor-linked molecules can be well-packed on electrode surfaces to reveal unidirectional orientation. Along this line, we have developed a variety of photovoltaic devices [11,12,18–20] consisting of the SAMs of porphyrin–fullerene-linked systems, which exhibit accelerated photoinduced charge separation (CS) and retarded charge recombination (CR) [18–23] as seen in photosynthesis. Although porphyrin–fullerene-linked systems have achieved a high quantum yield for CS in solution, it is still difficult to reflect the high value on a quantum yield of photocurrent generation using the SAMs of porphyrin–fullerene-linked systems [11,12,18–20]. Therefore, further systematic studies on the photoelectrochemical systems are required to disclose the controlling factors for photocurrent generation.

Here, we report novel SAMs of porphyrin–fullerene-linked dyads on ITO electrode aiming the development of molecular photovoltaic devices. C_{60} diacid is directly attached on the ITO surface to enhance electrical communication between the C_{60} moiety and the ITO electrode. The structures and photoelectrochemical properties have been examined in detail using spectroscopic and electrochemical methods.

2. Experimental

2.1. General

Melting points were recorded on a Yanagimoto micro-melting apparatus and are not corrected. ^{1}H NMR spectra were measured on a JEOL EX-270. Matrix-assisted laser

* Corresponding author. Fax: +81 75 383 2571.
E-mail address: imahori@scl.kyoto-u.ac.jp (H. Imahori).
[1] Co-corresponding author.
E-mail address: fukuzumi@chem.eng.osaka-u.ac.jp.

1010-6030/$ – see front matter © 2004 Elsevier B.V. All rights reserved.
doi:10.1016/j.jphotochem.2004.04.041

desorption/ionization (MALDI) time-of-flight mass spectra (TOF) were measured on a Kratos Compact MALDI I (Shimadzu). UV–vis spectra were obtained on a Shimadzu UV-3100 spectrometer. AFM measurements were performed in air with tapping mode using NanoScope IIIa (Veeco metrology group/ Digital Instruments). All solvents and chemicals were of reagent grade quality, purchased commercially and used without further purification unless otherwise noted. Tetrabutylammonium hexafluorophosphate used as a supporting electrolyte for the electrochemical measurements was obtained from Tokyo Kasei Organic Chemicals and recrystallized from methanol. Dry toluene and dry methylene chloride were heated at reflux and distilled from CaH_2. Thin-layer chromatography and flash column chromatography were performed with Alt. 5554 DC-Alufolien Kieselgel 60 F_{254} (Merck) and Fujisilica BW300, respectively. ITO electrode (190–200 nm ITO on transparent glass slides) was commercially available from Evers Inc. (Japan). The roughness factor ($R = 1.3$) was estimated by the AFM measurement with tapping mode.

2.2. Synthesis

1: A saturated solution of zinc acetate dihydrate in methanol (8 mL) was added to a solution of **2** [24] (64 mg, 50 μmol) in chloroform (50 mL) and refluxed for 5 h. After cooling, the reaction mixture was washed with saturated sodium bicarbonate aqueous solution and water successively, dried over anhydrous sodium sulfate, and then the solvent was removed under reduced pressure. **1** as a deep purple solid from chloroform–methanol (64 mg, 47 μmol, 95% yield): mp > 300 °C; ^{1}H NMR ($CDCl_3$) δ 1.53 (s, 36H), 4.10 (s, 5H), 4.35 (s, 2H), 4.69 (s, 2H), 7.58 (d, $J = 7$ Hz, 2H), 7.75 (d, $J = 7$ Hz, 2H), 7.82 (s, 2H), 8.02 (s, 4H), 8.09 (d, $J = 2$ Hz, 4H), 8.13 (s, 1H), 8.28 (d, $J = 7$ Hz, 2H), 8.29 (d, $J = 7$ Hz, 2H), 8.33 (s, 1H), 8.38 (d, $J = 7$ Hz, 2H), 8.40 (d, $J = 7$ Hz, 2H), 8.91 (d, $J = 5$ Hz, 2H), 8.94 (d, $J = 5$ Hz, 2H), 9.04 (d, $J = 5$ Hz, 2H), 10.02 (s, 1H); ^{13}C NMR ($CDCl_3$) δ 191.00, 165.95, 150.63, 150.49, 150.36, 149.38, 148.56, 147.67, 143.62, 141.67, 134.80, 133.19, 132.65, 132.48, 132.32, 131.33, 131.09, 129.67, 129.59, 125.31, 123.06, 122.72, 120.88, 119.70, 118.56, 35.04, 31.75; MALDI-TOFMASS (positive mode) m/z 1352 ($M + H^+$); Anal. Calcd. for $C_{76}H_{83}N_5O_3Zn(H_2O)$ (FW 1197.9): C, 76.20; H, 7.15; N, 5.85. Found: C, 75.76; H, 7.27; N, 5.49.

2.3. Cyclic voltammetry measurements

All electrochemical studies were performed on a Bioanalytical Systems Inc., CV-50 W voltammetric analyzer using a standard three-electrode cell with a modified ITO working electrode (electrode area, 0.48 cm^2), a platinum wire counter electrode, and an Ag/AgCl (sat. KCl) reference electrode in CH_2Cl_2 containing 0.2 M n-Bu_4NPF_6 electrolyte with a sweep rate of 0.10 V s^{-1}. The adsorbed amounts of compounds were determined from the charges of the anodic peak of the porphyrin first oxidation or those of the cathodic peak of the fullerene first reduction.

2.4. Photoelectrochemical measurements

Photoelectrochemical measurements were performed in a one-compartment Pyrex UV cell (5 mL). The cell was illuminated with monochromatic excitation light through interference filters (MIF-S, Vacuum Optics Corporation of Japan) by a 180 W UV lamp (Sumida LS-140 V) or a monochromator (Ritsu MC-10N) by a 500 W xenon lamp (Ushio XB-50101AA-A) on the SAM of 0.48 cm^2. The photocurrent was measured in a three-electrode arrangement (Bioanalytical Systems Inc., CV-50W), a modified ITO working electrode (electrode area, 0.48 cm^2), a platinum wire counter electrode (the distance between electrodes is 0.3 mm), and a Ag/AgCl (sat. KCl) reference electrode. The light intensity was monitored by an optical power meter (Anritsu ML9002A) and corrected. Quantum yields were calculated based on the number of photons absorbed by the chromophore on the ITO electrodes at each wavelength using the input power, the photocurrent density, and the absorbance determined from the absorption spectrum on the ITO electrode.

3. Results and discussion

3.1. Preparation and characterization

The SAMs of porphyrin–fullerene dyads on the ITO electrode have been prepared to reveal efficient photocurrent generation on the ITO electrode. The investigated systems are shown in Fig. 1. Their photoelectrochemical and photodynamical properties are compared to those of corresponding porphyrin–fullerene dyads (ZnP-C_{60} and H_2P-C_{60} [24]) in solution to disclose the difference.

The general strategy employed for synthesizing the SAMs is summarized in Scheme 1. ITO electrodes were immersed into 1 mM bromobenzene solution of $C_{61}(COOH)_2$ in the presence of DCC (dicyclohexylcarbodiimide) and BtOH (1H-benzotriazol-1-ol), and stirred at room temperature for 40 h. Then, the modified ITO electrodes were washed well and sonicated in bromobenzene for 2 min to give C_{60}-ref/ITO [25]. Zincporphyrin aldehyde **1** or freebase porphyrin aldehyde **2** [24] was coupled to C_{60}-ref/ITO by refluxing in the presence of N-methylglycine for 3 days in toluene to yield ZnP-C_{60}/ITO or H_2P-C_{60}/ITO. Porphyrin–fullerene dyads (ZnP-C_{60} and H_2P-C_{60}) were obtained by following the same procedures as described previously [24].

Fig. 2a displays the absorption spectra of ZnP-C_{60}/ITO and porphyrin reference ZnP-C_{60} measured in THF. The Soret band of ZnP-C_{60}/ITO becomes broader than that of ZnP-C_{60} in THF. The λ_{max} value of the Soret band of

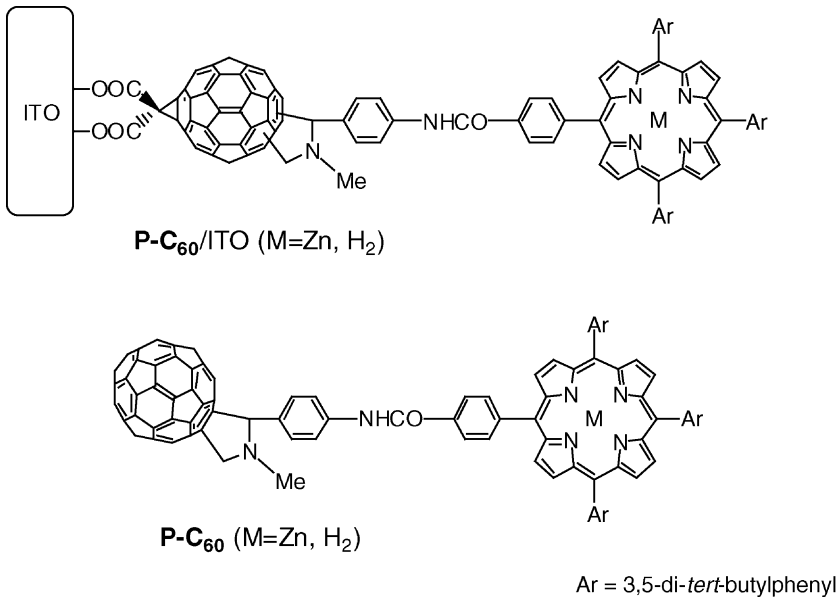

Fig. 1. Self-assembled monolayers of porphyrin–fullerene dyads on ITO and porphyrin–fullerene references.

ZnP-C_{60}/ITO (430 nm) is red-shifted by 4 nm as compared to that of ZnP-C_{60} in THF (426 nm). This indicates that the porphyrin environments on ITO are similar and perturbed moderately within the monolayers, as compared to the reference in THF, due to the aggregation [11,12]. Similar broadening and red-shift of the Soret band was noted for H_2P-C_{60}/ITO (Fig. 2b).

The cyclic voltammetry measurements of ZnP-C_{60}/ITO, H_2P-C_{60}/ITO, and C_{60}-ref/ITO in CH_2Cl_2 containing 0.2 M *n*-Bu_4NPF_6 were performed with a sweep rate of 0.10 V s^{-1} (electrode area, 0.48 cm^{-2}) to estimate the surface coverage, as shown in Fig. 3. The adsorbed amount (Γ) of C_{60} on C_{60}-ref/ITO was calculated from the first cathodic peak current of the C_{60} as 2.1×10^{-10} mol cm^{-2} using the roughness factor of 1.3 for ITO electrode from atomic force microscopy (AFM) measurements. This value is in good agreement of the well-packed surface coverage for C_{60} SAM on electrodes ($1.9–2.0 \times 10^{-10}$ mol cm^{-2}) [26]. The adsorbed amounts

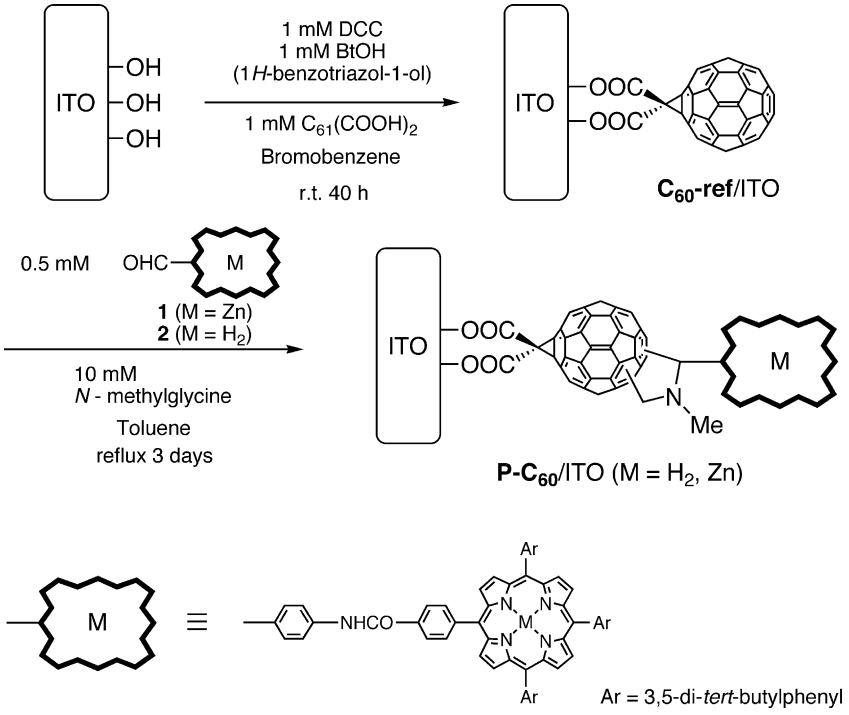

Scheme 1.

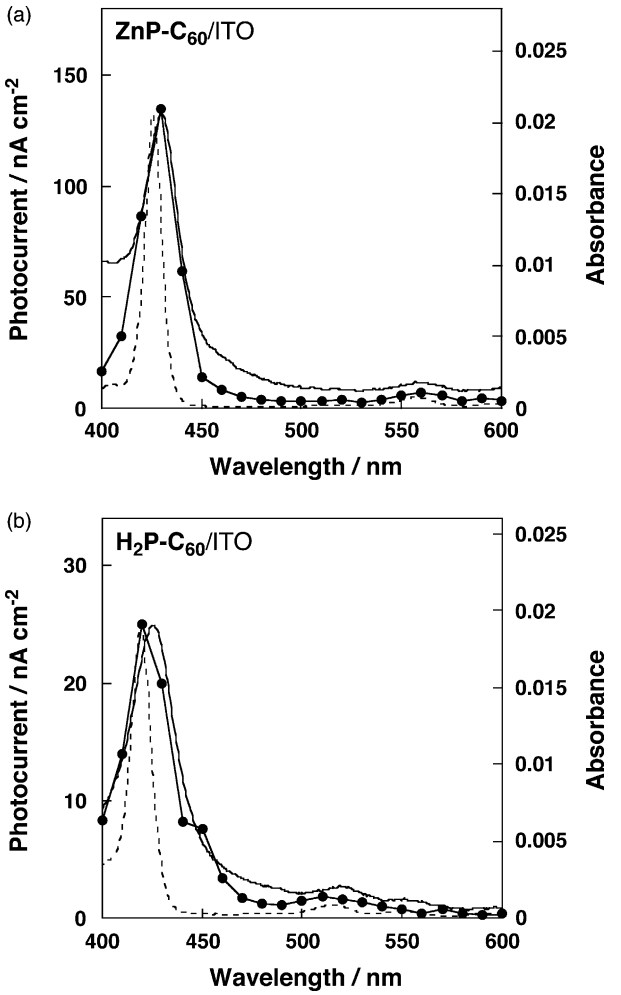

Fig. 2. (a) Absorption spectra of ZnP-C_{60}/ITO (solid line) and ZnP-C_{60} in THF (dashed line) and the action spectrum of ITO/ZnP-C_{60}/AsA/Pt system (solid line with closed circles); applied potential: +0.10 V vs Ag/AgCl (sat. KCl). (b) Absorption spectra of H_2P-C_{60}/ITO (solid line) and H_2P-C_{60} in THF (dashed line) and the action spectrum of ITO/H_2P-C_{60}/AsA/Pt system (solid line with closed circles); applied potential: +0.10 V vs Ag/AgCl (sat. KCl). $\lambda_{ex} = 430$ nm for zincporphyrin and $\lambda_{ex} = 420$ nm for freebase porphyirn (500 $\mu W\,cm^{-2}$); an argon-saturated 0.1 M Na_2SO_4 aqueous solution containing 50 mM AsA.

(Γ) of porphyrin on ZnP-C_{60}/ITO and H_2P-C_{60}/ITO were also calculated from the first anodic peak currents of the porphyrin as 2.8×10^{-11} mol cm^{-2} and 6.8×10^{-11} mol cm^{-2}, respectively. Relative molar ratio of porphyrin versus C_{60} is about 1:8 for ZnP-C_{60}/ITO and 1:3 for H_2P-C_{60}/ITO. This indicates that only a part of C_{60} molecules on the ITO can react with porphyrin molecules due to the steric hindrance and the poor reactivity on the C_{60} surface.

AFM measurements were performed for the modified ITO surfaces to obtain the information on the surface structures. AFM images of C_{60}-ref/ITO and ITO itself reveal rather smooth surface, whereas ZnP-C_{60}/ITO and H_2P-C_{60}/ITO exhibit small domain structures with 10–20 nm size, which presumably corresponds to the porphyrin aggregates on the C_{60} surface (Fig. 4).

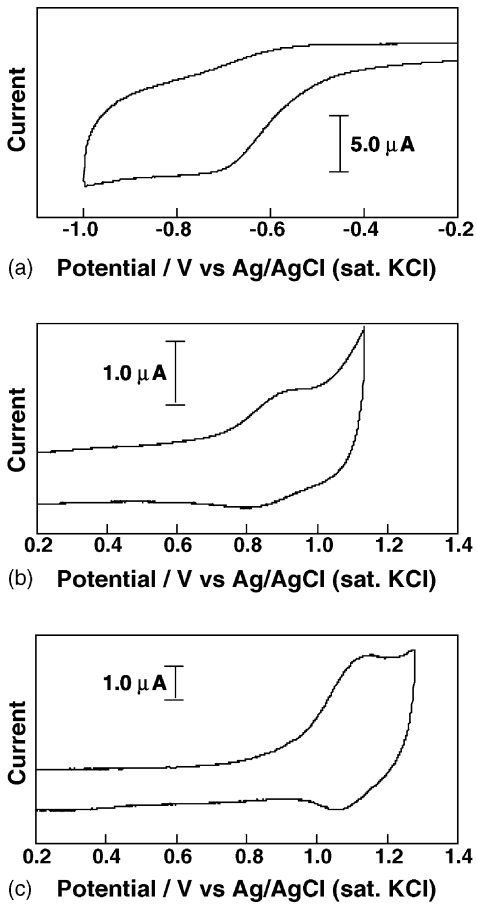

Fig. 3. Cyclic voltammograms of (a) C_{60}-ref/ITO, (b) ZnP-C_{60}/ITO, and (c) H_2P-C_{60}/ITO in CH_2Cl_2 containing 0.2 M *n*-Bu_4NPF_6 with a sweep rate of 0.1 V s^{-1}, electrode area, 0.48 cm^2; counter electrode, Pt wire; reference electrode, Ag/AgCl (sat. KCl).

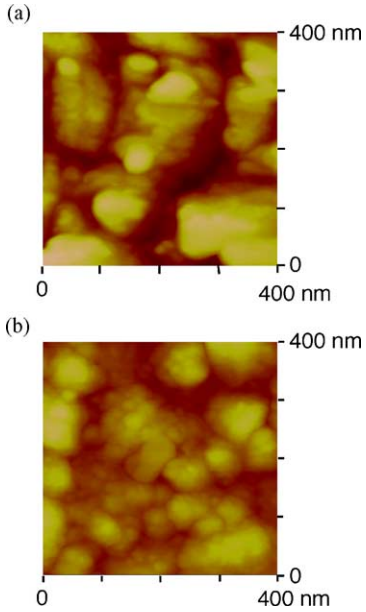

Fig. 4. Tapping mode atomic force micrography of: (a) C_{60}-ref/ITO (*Z* range: 25 nm) and (b) ZnP-C_{60}/ITO in air (*Z* range: 50 nm). The color scale represents the height topography, with bright and dark representing the highest and lowest features, respectively.

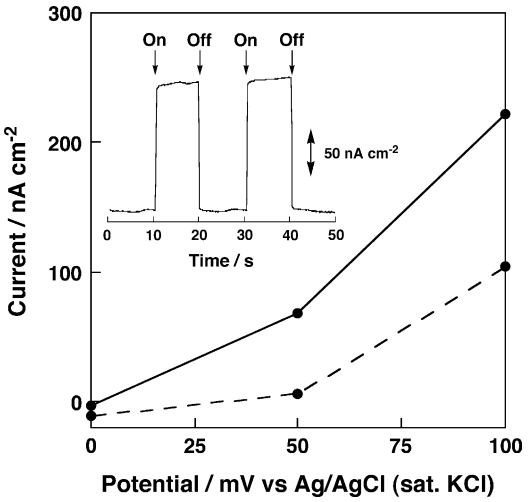

Fig. 5. Photocurrent vs. applied potential curves for the ITO/ZnP-C_{60}/AsA/Pt system (solid line with closed circles). The dark current is shown as dotted line with closed circles. $\lambda_{ex} = 430$ nm (500 μW cm^{-2}); an argon-saturated 0.1 M Na_2SO_4 aqueous solution containing 50 mM AsA.

3.2. Photoelectrochemical properties

Photoelectrochemical measurements were carried out in an argon-saturated 0.1 M Na_2SO_4 aqueous solution containing 50 mM ascorbic acid (AsA) acting as an electron sacrificer using ZnP-C_{60}/ITO or H_2P-C_{60}/ITO as the working electrode, a platinum counter electrode, and an Ag/AgCl (sat. KCl) reference electrode (hereafter, represented by ITO/ZnP-C_{60} or H_2P-C_{60}/AsA/Pt, where / denotes an interface). When ZnP-C_{60}/ITO electrode was irradiated with $\lambda_{ex} = 430$ nm light with a power density of 500 μW cm^{-2} at applied potential of +0.10 V versus Ag/AgCl (sat. KCl), a stable anodic photocurrent from the electrolyte to the ITO electrode appeared, as shown in Fig. 5. The photocurrent fell down instantly when the illumination was cut off. The anodic photocurrent increases monotonically with increasing positive bias to the ITO electrode [from 0 to +0.10 V versus Ag/AgCl (sat. KCl), as shown in Fig. 5. The action spectrum largely agrees with the absorption spectrum of ZnP-C_{60}/ITO in 400–600 nm (Fig. 2a), implying that the porphyrin is the photoactive species responsible for the photocurrent generation. Similar photoelectrochemical behavior was observed for the ITO/H_2P-C_{60}/AsA/Pt system. These results demonstrate that photocurrent flows from the electrolyte to the ITO electrode via the excited state of the porphyrin SAM. The quantum yield of photocurrent generation was determined for ITO/ZnP-C_{60}/AsA/Pt and ITO/H_2P-C_{60}/AsA/Pt systems at applied potential of +0.10 V versus Ag/AgCl (sat. KCl). The internal quantum yield (ϕ) based on the number of photons absorbed by the chromophores was calculated using the input power ($\lambda_{ex} = 430$ nm for zincporphyrin and $\lambda_{ex} = 420$ nm for freebase porphyrin, light of 500 μW cm^{-2}), the photocurrent density, and the absorbance on the electrodes (ITO/ZnP-C_{60}/AsA/Pt system: $i = 135$ nA cm^{-2}, $A = 0.015$; ITO/H_2P-C_{60}/AsA/Pt system: $i = 25$ nA cm^{-2}, $A = 0.019$). The ϕ value of ITO/ZnP-C_{60}/AsA/Pt system (2.5%) is larger by a factor of 6 than the value of ITO/H_2P-C_{60}/AsA/Pt system (0.4%).

Based on the above results together with the well-established photodynamics of porphyrin–fullerene-linked systems on electrodes as well as those of ZnP-C_{60} and H_2P-C_{60} in solution [11,12,18–20], the mechanism of photocurrent generation in the ITO/ZnP-C_{60}/AsA/Pt and ITO/H_2P-C_{60}/AsA/Pt systems is summarized in Scheme 2. First, an intramolecular ET takes place from ^{1}ZnP* [−1.20 V versus Ag/AgCl (sat. KCl)] or $^1H_2P^*$ [−0.79 V versus Ag/AgCl (sat. KCl)] to C_{60}, followed by intermolecular ET from AsA [+0.29 V versus Ag/AgCl (sat. KCl)] to the porphyrin radical cation ZnP$^{\bullet+}$ [+0.85 V versus Ag/AgCl

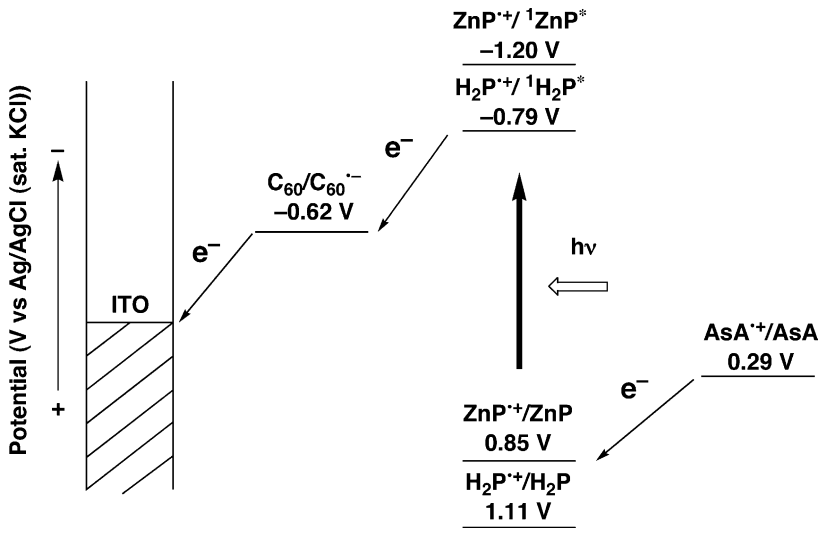

Scheme 2.

(sat. KCl)] or $H_2P^{\bullet+}$ [1.11 V versus Ag/AgCl (sat. KCl)], yielding the C_{60} radical anion ($C_{60}^{\bullet-}$) and AsA radical cation ($AsA^{\bullet+}$). Photogenerated $C_{60}^{\bullet-}$ [−0.62 V versus Ag/AgCl (sat. KCl)] gives an electron to the ITO electrode, leading to the anodic photocurrent generation. The quantum yields of charge separation of ZnP-C_{60} (99%) and H_2P-C_{60} (98%) [24] in benzonitrile are virtually the same on a basis of results obtained by using pico- and nanosecond transient absorption measurements. The lifetime of charge-separated state of ZnP-C_{60} (770 ns) in benzonitrile becomes longer than that of H_2P-C_{60} (45 ns) in the same solvent. This clearly demonstrates that the long-lived charge-separated state as well as the charge separation efficiency is an important controlling factors for achieving a high quantum yield of photocurrent generation in the donor–acceptor-linked system which is covalently attached to ITO surface.

4. Conclusion

We have successfully constructed molecular photovoltaic devices using self-assembled monolayers of porphyrin–fullerene-linked dyads on ITO electrodes. The high quantum yield (99%) and the long lifetime (770 ns) of the charge-separated state of the zincporphyrin–fullerene dyad in solution play essential roles on achieving a high quantum yield of photocurrent generation in donor–acceptor-linked system which is covalently attached to ITO surface.

Acknowledgements

This work was supported by Grant-in-Aids for 21st Century COE on Kyoto University Alliance for Chemistry and Scientific Research from the Ministry of Education, Science, Sports and Culture, Japan.

References

[1] J.-F. Eckert, J.-F. Nicoud, J.-F. Nierengarten, S.-G. Liu, L. Echegoyen, F. Barigelletti, N. Armaroli, L. Ouali, V. Krasnikov, G. Hadziioannou, J. Am. Chem. Soc. 122 (2000) 7467.
[2] E. Peeters, P.A. van Hal, J. Knol, C.J. Brabec, N.S. Sariciftci, J.C. Hummelen, R.A.J. Janssen, J. Phys. Chem. B104 (2000) 10174.
[3] R. Argazzi, C.A. Bignozzi, T.A. Heimer, F.N. Castellano, G.J. Meyer, J. Am. Chem. Soc. 117 (1995) 11815.
[4] P. Bonhote, J.-E. Moser, R. Humphry-Baker, N. Vlachopoulos, S.M. Zakeeruddin, L. Walder, M. Grätzel, J. Am. Chem. Soc. 121 (1999) 1324.
[5] C.J. Kleverlaan, M.T. Indelli, C.A. Bignozzi, L. Pavanin, F. Scandola, G.M. Hasselman, G.J. Meyer, J. Am. Chem. Soc. 122 (2000) 2840.
[6] N.V. Tkachenko, E. Vuorimaa, T. Kesti, A.S. Alekseev, A.Y. Tauber, P.H. Hynninen, H. Lemmetyinen, J. Phys. Chem. B104 (2000) 6371.
[7] C. Luo, D.M. Guldi, M. Maggini, E. Menna, S. Mondini, N.A. Kotov, M. Prato, Angew. Chem. Int. Ed. 39 (2000) 3905.
[8] M. Lahav, V. Heleg-Shabtai, J. Wasserman, E. Katz, I. Willner, H. Dürr, Y.-Z. Hu, S.H. Bossmann, J. Am. Chem. Soc. 122 (2000) 11480.
[9] K. Uosaki, T. Kondo, X.-Q. Zhang, M. Yanagida, J. Am. Chem. Soc. 119 (1997) 8367.
[10] A. Ikeda, T. Hatano, S. Shinkai, T. Akiyama, S. Yamada, J. Am. Chem. Soc. 123 (2001) 4855.
[11] H. Imahori, H. Norieda, H. Yamada, Y. Nishimura, I. Yamazaki, Y. Sakata, S. Fukuzumi, J. Am. Chem. Soc. 123 (2001) 100.
[12] H. Yamada, H. Imahori, Y. Nishimura, I. Yamazaki, T.K. Ahn, S.K. Kim, D. Kim, S. Fukuzumi, J. Am. Chem. Soc. 125 (2003) 9129.
[13] M. Fujihira, K. Nishiyama, H. Yamada, Thin Solid Films 132 (1985) 77.
[14] M. Fujihira, M. Sakomura, T. Kamei, Thin Solid Films 180 (1989) 43.
[15] P. Seta, E. Bienvenue, A.L. Moore, P. Mathis, R.V. Bensasson, P.A. Liddell, P.J. Pessiki, A. Joy, T.A. Moore, D. Gust, Nature 316 (1985) 653.
[16] G. Steinberg-Yfrach, J.-L. Rigaud, E.N. Durantini, A.L. Moore, D. Gust, T.A. Moore, Nature 392 (1998) 479.
[17] A. Ulman (Ed.), Introduction to Ultrathin Organic Films, Academic Press, San Diego, 1991.
[18] H. Imahori, Y. Sakata, Adv. Mater. 9 (1997) 537.
[19] H. Imahori, Y. Sakata, Eur. J. Org. Chem. 10 (1999) 2445.
[20] H. Imahori, Y. Mori, Y. Matano, J. Photochem. Photobiol. C 4 (2003) 51.
[21] H. Imahori, K. Hagiwara, M. Aoki, T. Akiyama, S. Taniguchi, T. Okada, M. Shirakawa, Y. Sakata, Chem. Phys. Lett. 263 (1996) 545.
[22] H. Imahori, N.V. Tkachenko, V. Vehmanen, K. Tamaki, H. Lemmetyinen, Y. Sakata, S. Fukuzumi, J. Phys. Chem. A 105 (2001) 1750.
[23] H. Imahori, H. Yamada, D.M. Guldi, Y. Endo, A. Shimomura, S. Kundu, K. Yamada, T. Okada, Y. Sakata, S. Fukuzumi, Angew. Chem. Int. Ed. 41 (2002) 2344.
[24] H. Imahori, K. Tamaki, D.M. Guldi, C. Luo, M. Fujitsuka, O. Ito, Y. Sakata, S. Fukuzumi, J. Am. Chem. Soc. 123 (2001) 2607.
[25] T.-X. Wei, J. Zhai, J.-H. Ge, L.-B. Gan, C.-H. Huang, G.-B. Luo, L.-M. Ying, T.-T. Liu, X.-S. Zhao, Appl. Surf. Sci. 151 (1999) 153.
[26] X. Shi, W.B. Caldwell, K. Chen, C.A. Mirkin, J. Am. Chem. Soc. 116 (1994) 11598.